Design and implementation of conventional and advanced controllers for magnetic bearing system stabilization

Juan Shi and Wee Sit Lee
School of Engineering and Science, Victoria University
Australia

1. Introduction

Active magnetic bearings (AMBs) employ electromagnets to support machine components. The magnetic forces are generated by feedback controllers to suspend the machine components within the magnetic field and to control the system dynamics during machine operation. AMBs have many advantages over mechanical and hydrostatic bearings. These include zero frictional wear and efficient operation at extremely high speed. They are also ideal for clean environments because no lubrication is required. Hence, as a result of minimal mechanical wears and losses, system maintenance costs of AMBs are low. AMBs are used in a number of applications such as energy storage flywheels, high-speed turbines and compressors, pumps and jet engines (Williams et al., 1990), (Lee et al., 2006). AMBs are inherently unstable and it is necessary to use feedback control system for stabilization (Williams et al., 1990), (Bleuler et al., 1994). This can be achieved by sensing the position of the rotor and using feedback controllers to control the currents of the electromagnets.

This chapter will present our experience in different design approaches of stabilizing magnetic bearing systems. By using these approaches, feedback controllers will be designed and implemented for an experimental magnetic bearing system - the MBC500 magnetic bearing system (Magnetic Moments, 1995).

As most of the design methods to be presented are model based, a plant model is required. Since the magnetic bearing system is open-loop unstable, a closed-loop system identification procedure is required to identify its model. For this purpose, we adopted a two step closed-loop system identification procedure in the frequency domain. After various model structures were attempted, an 8^{th}-order model of the MBC500 magnetic bearing system was identified by applying the System ID toolbox of MatLab to the collected frequency response data. In the following, this 8^{th}-order unstable model will be treated as the full-order model of the open-loop plant.

In the first approach, a model based conventional controller is designed on the basis of a reduced 2^{nd}-order unstable model of the MBC500 magnetic bearing system. In this approach, notch filters are necessary to cancel the resonant modes of the active magnetic bearing system (Shi & Revell, 2002).

In the second approach, a model based controller is designed via interpolation of units on the complex s-plane. This is an analytical design method. Among various approaches for feedback control design, analytical design methods offer advantages over trial and error design techniques. These include the *conditions for the existence of a solution* and *the algorithms that are guaranteed to find the solutions, when these exist (*Dorato, 1999). A limitation of the analytical methods is, however, that they tend to generate more complex controllers. One of the analytical feedback controller design methods is the *interpolation approach* we employed, where units in the algebra of bounded-input bounded-output (BIBO) stable proper rational functions are used to interpolate specified values at some given points in the complex s-domain (Dorato, 1999), (Dorato,1989). When applying this approach to stabilize the MBC500 magnetic bearing system, the controller is designed on the basis of the reduced 2^{nd}-order unstable model. Since there are resonant modes that can threaten the stability of the closed loop system, notch filters are employed to help secure stability (Shi and Lee, 2009).

The third approach in this chapter involves the design of a Fuzzy Logic Controller (FLC). The FLC uses error and rate of change of error in the position of the rotor as inputs and produces output voltages to control the currents of the amplifiers that driving the magnetic bearing system. This approach does not require any analytical model of the MBC500 magnetic bearing system. This can greatly simplify the controller design process. Furthermore, it will be demonstrated that the FLC can stabilize the magnetic bearing system without the use of any notch filter (Shi et al., 2008) (Shi & Lee, 2009). Instead of applying the output of a FLC directly to the input of a magnetic bearing system (like what we have done here), the output of a FLC can also be used to tune the gains of controllers. For example, Habib and Inayat-Hussain (2003) reported a dual active magnetic bearing system in which the output of a FLC was used to tune the gains of a linear PD controller.

The performance of each of the controllers described above will be tested first via simulation. They will be compared critically in terms closed-loop step responses (steady-state error, peak overshoot, and settling time), disturbance rejection, and the size of control signal. The controllers designed will then be coded in C and implemented in real time on a Digital Signal Processor (DSP) card. The implementation results will also be compared with the simulation results.

2. Description of the MBC500 Magnetic Bearing System

The MBC500 magnetic bearing system consists of two active radial magnetic bearings which support a rotor. It is mounted on top of an anodized aluminium case as shown in Figure 1 (Magnetic Moments, 1995). The rotor shaft is actively positioned in the radial directions at the shaft ends (four degrees of freedom). It is passively centred in the axial direction and can freely rotate about its axial axis. The system employs four linear current-amplifier pairs (one pair for each radial bearing axis) and four internal analogue lead compensators to independently control the radial bearing axes. In this chapter, we shall present design examples where all the four on-board analogue controllers will be replaced by digital controllers designed through different approaches.

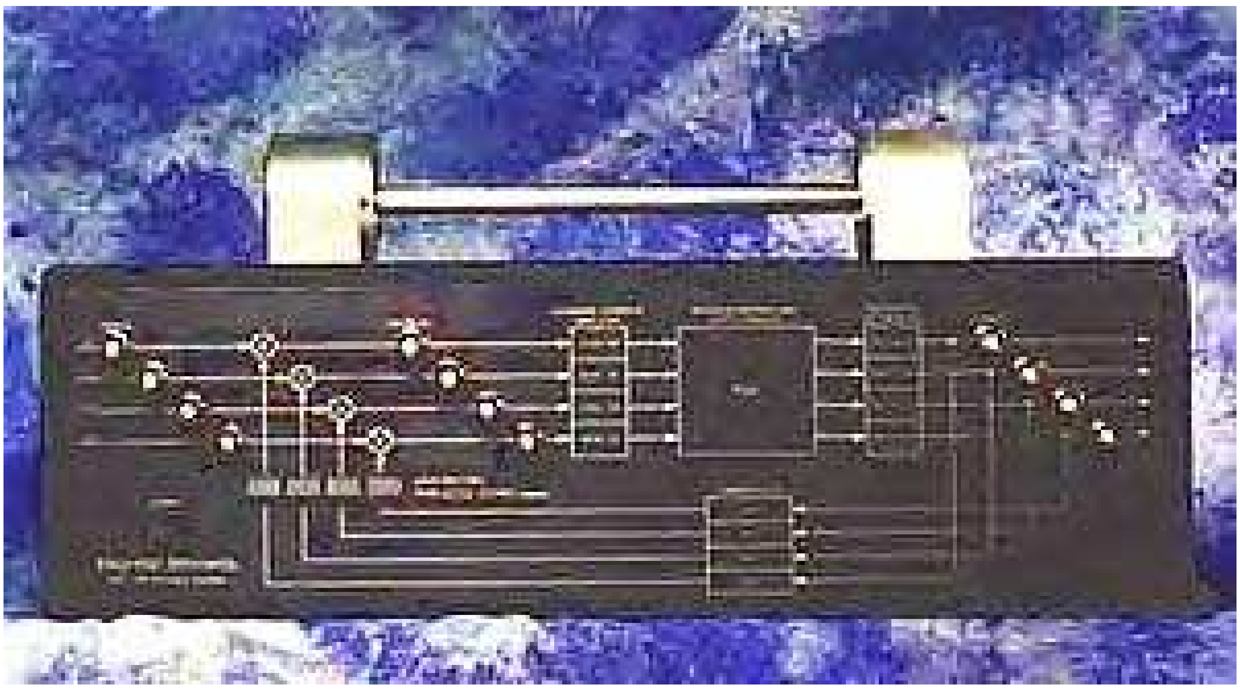

Fig. 1. MBC500 magnetic bearing research experiment (Source: Magnetic Moments, 1995)

A diagram which defines the system coordinates is shown in Figure 2. The system has four degrees of freedom, with two degrees of freedom at each end. These degrees of freedom are all translational in nature and are perpendicular to the z-axis. They are in the horizontal direction (x_1 and x_2) and in the vertical direction (y_1 and y_2) (Magnetic Moments, 1995).

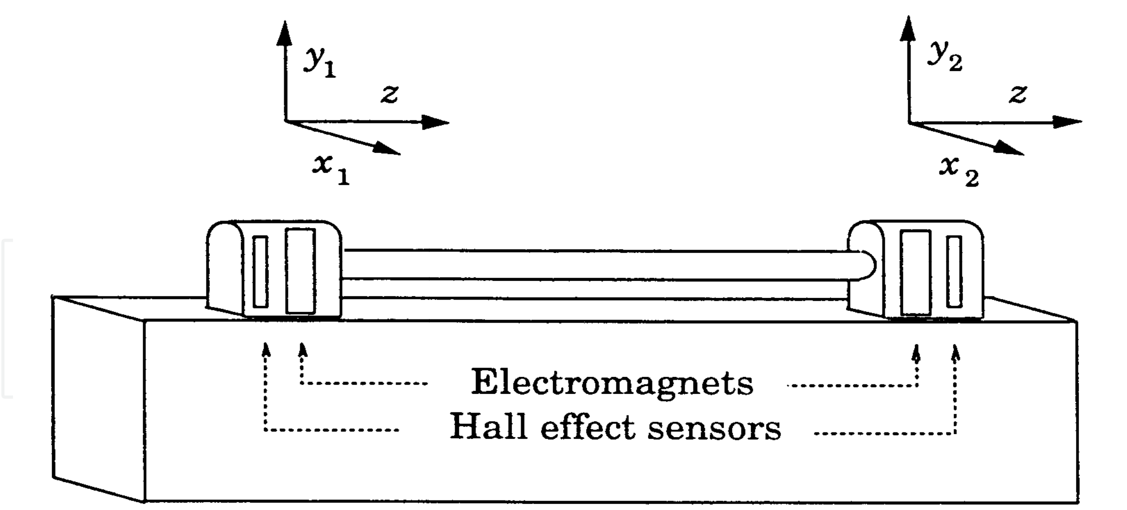

Fig. 2. MBC500 system configurations (Morse, 1996)

3. System Identification

3.1 System Identification and reduced order model

Since the magnetic bearing system is open-loop unstable, a closed-loop system identification procedure was required to identify its model. For this purpose, we adopted a two-step closed-loop system identification procedure (Morse 1996), (Van den Hof & Schrama 1993). The procedure employs frequency response data. The details of the frequency response experiment and the system identification procedure were described in (Shi & Revell, 2002).

Various model structures were attempted before an 8th-order final model was found. The transfer function of the 8th-order model is shown as follows:

$$P(s) = \frac{-104.21(s-2854)(s^2+9785s+3.274\times10^7)(s^2-379.15s+2.048\times10^7)(s^2-564.5s+1.645\times10^8)}{(s+511)(s-292.7)(s^2+32.97s+2.344\times10^7)(s^2+6197s+4.02\times10^7)(s^2+23.77s+1.66\times10^8)} \quad (1)$$

Note that the pole at s=292.7 of the above transfer function indicates the instability of the open-loop MBC500 magnetic bearing system. Furthermore, it should be noted that when the model is employed for model-based controller design, closed-loop performance limitations will also be imposed by the right-half plane zero at s=2854 (Freudenberg & Looze, 1985).
It can be seen from equation (1) that the MBC500 magnetic bearing model includes two resonant modes. They are located at approximately 780 Hz and 2055 Hz. Each of these two modes causes an increase in magnitude and a large change in phase in the frequency response. These characteristics of the resonant modes can threaten the stability of the closed-loop system. Consequently, two notch filters are designed to eliminate these unwanted resonances. Since the notch filters must cancel out the resonant modes, the resonant frequencies of the experimental model must be obtained accurately. Two elliptic notch filters have been designed to notch out the resonant modes. As a result, controllers can be designed on the basis of a reduced order unstable system model where the resonant modes are absent. This reduced order model of the plant can be obtained by eliminating the resonant modes and preserving the DC gain of the 8th-order magnetic bearing system model. The resulting reduced order model has a transfer function of

$$P(s) = \frac{-75.86(s-2854)}{(s+511)(s-292.7)} \quad (2)$$

4. Conventional Controller Design

A single-loop unity-feedback control system shown in Figure 3 is considered in the controller design in this chapter. In this Figure, P(s) is the transfer function of the magnetic bearing system and C(s) is the transfer function of the controller.

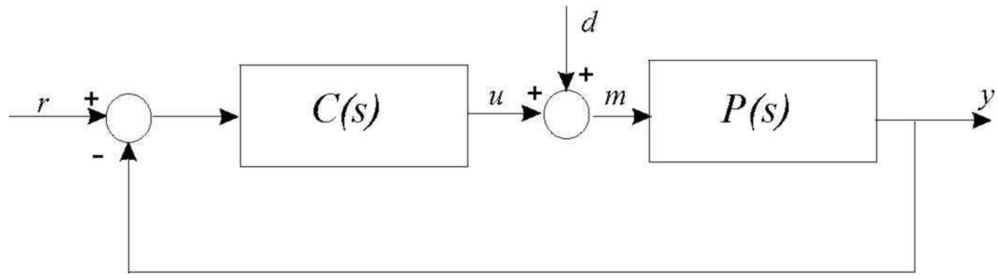

Fig. 3. A single-loop unity-feedback control system

On the basis of the reduced order model described by equation (2), a conventional lead compensator was designed by using root locus method (Shi & Revell, 2002). Although the lead compensator has been designed to stabilize the MBC500 magnetic bearing system, its frequency response has a magnitude which remains large in the high frequency region. This will affect the stability robustness of the closed-loop system. Thus an additional high frequency pole at 7000 Hz (or 43982 rad/s) was incorporated to reduce the gain at high frequency. As a result, the final controller employed in (Shi & Revell, 2002) was a second order controller (lead with low pass filter with cut off frequency of 7000 Hz) and the transfer function of the controller is as follows:

$$C_{lead}(s) = \frac{4.23(s + 1067.3)}{(s + 3202)} \frac{43982}{(s + 43982)} \quad (3)$$

Figure 4 illustrates the root locus of the magnetic bearing system represented by the reduced order model shown in equation (2) with the designed lead compensator shown in equation (3). The closed-loop poles are at -4.43×10^4, -2.73×10^3, and -167±392j respectively. Figure 5 shows the Bode plot of the closed-loop system with and without the added low pass filter. It can be seen from the Bode plot that the added low pass filter improves the system robustness by reducing system sensitivity to uncertain high frequency dynamics.

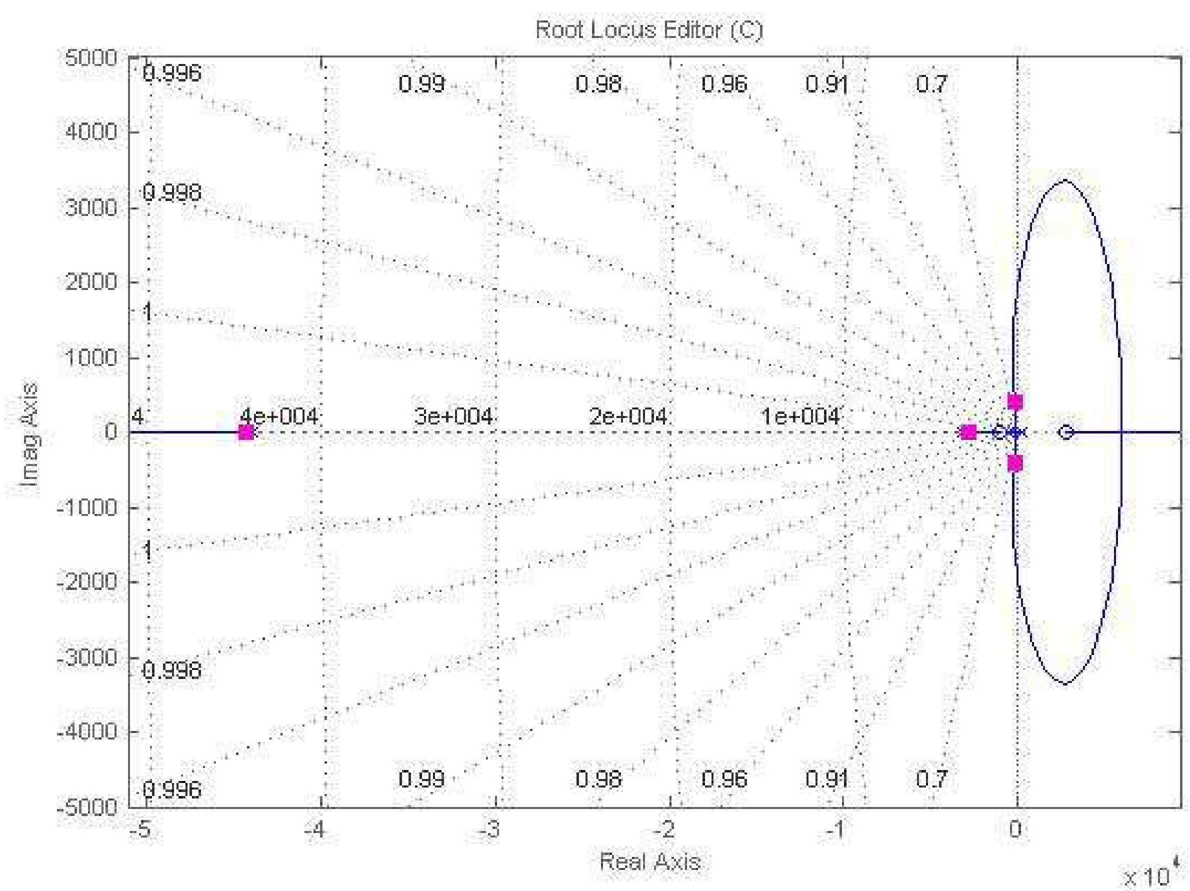

Fig. 4. Root locus of the magnetic bearing system (a reduced 2nd-order model is used here) with the designed lead compensator

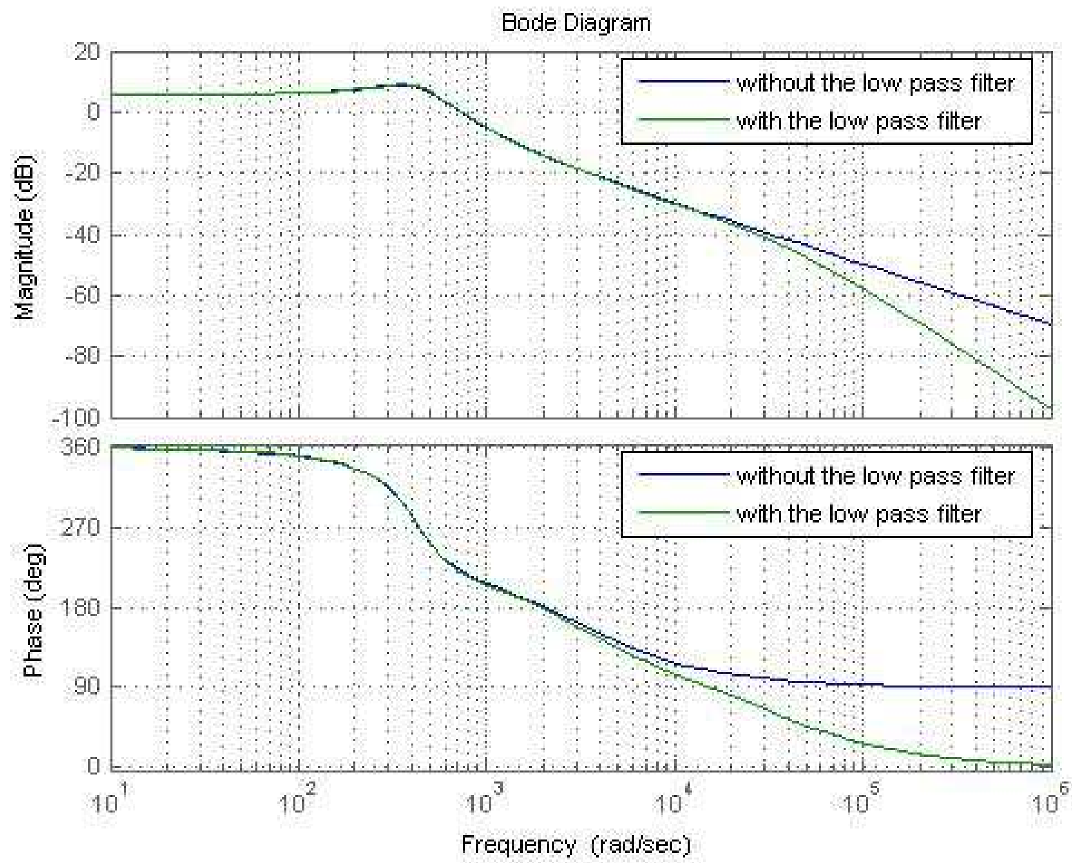

Fig. 5. Bode plot of the magnetic bearing system (a reduced 2nd-order model is used here) with the designed lead compensator

5. Controller Design via Interpolation Approach

5.1 Controller Design via Interpolation Approach

A single-loop unity-feedback control system shown in Figure 3 is considered in the controller design via the interpolation approach described in (Dorato, 1999). It was shown in (Dorato, 1999) that any rational transfer function,

$$P(s) = \frac{n_p(s)}{d_p(s)} \tag{4}$$

where $n_p(s)$ and $d_p(s)$ are arbitrary polynomials, can always be written as a ratio of two coprime *stable* proper transfer functions,

$$P(s) = \frac{N_p(s)}{D_p(s)} \tag{5}$$

where

$$N_p(s) = \frac{n_p(s)}{h(s)} \tag{6}$$

and

$$D_p(s) = \frac{d_p(s)}{h(s)} \quad (7)$$

with $h(s)$ a Hurwitz polynomial of appropriate degree. Let $U(s)$ be a *unit* in the algebra of BIBO stable proper transfer functions, then following (Dorato, 1999) a stable stabilizing controller can be calculated as:

$$C(s) = \frac{U(s) - D_p(s)}{N_p(s)} \quad (8)$$

when P(s) satisfies the parity-interlacing property (p.i.p.) condition (Youla, 1974) and U(s) satisfies certain interpolation conditions. Specifically, let b_i denotes the zeros of the plant in the RHP, the closed-loop system will be internally stable, and the controller will be stable, if and only if $U(s)$ interpolates to $U(b_i) = D_p(b_i)$ (Dorato, 1999).

5.2 Controller Design for the Magnetic Bearing System

Firstly we note that the reduced order model of the plant described by equation (2) has a zero at s =2854 and a zero at $s = \infty$. Since the pole at s = 292.7 is not between these two zeros, the *parity-interlacing property* (p.i.p.) condition (Youla, 1974) is satisfied and a stable stabilizing controller is known to exist.

In the following, we assume that the design must satisfy the following specifications:

- The sensitivity function is to have all its poles at s =-511,
- A steady-state error magnitude (subjected to a unit step input) of $e_{ss} = 0.1$.

Since the closed-loop transfer functions are:

$$\frac{E(s)}{R(s)} = \frac{1}{1 + C(s)P(s)} = \frac{D_p(s)}{U(s)} \quad (9)$$

$$\frac{Y(s)}{D(s)} = \frac{P(s)}{1 + C(s)P(s)} = \frac{N_p(s)}{U(s)} \quad (10)$$

$$\frac{M(s)}{R(s)} = \frac{C(s)}{1 + C(s)P(s)} = \frac{D_p(s)C(s)}{U(s)} \quad (11)$$

By choosing $h(s) = (s + 511)^2$, the requirement of the closed-loop poles specification will be satisfied. As a result,

$$N_p(s) = \frac{-75.86(s - 2854)}{(s + 511)^2} \quad (12)$$

and

$$D_p(s) = \frac{(s - 292.7)}{(s + 511)^2} \quad (13)$$

The interpolation conditions are:

$U(2854) = D_p(2854) = 0.7612$, and $U(\infty) = D_p(\infty) = 1$.

Let the steady-state error magnitude be $e_{ss} = 0.1$, then:

$$e_{ss} = \left|\frac{D_p(0)}{U(0)}\right| \tag{14}$$

Let the interpolating unit $U(s)$ take of the following form:

$$U(s) = \frac{h(s)}{s^2 + as + b} \tag{15}$$

with $a > 0$ and $b > 0$, then after some simple calculations, the controller is found to be:

$$C(s) = \frac{6.8046(s + 511)(s + 99.59)}{(s + 2322)(s + 19.73)} \tag{16}$$

Controllers with other values of steady-state error magnitude can also be found by following similar procedures. For example, the following controllers $C_1(s)$ and $C_2(s)$ were computed on the basis of error magnitude $e_{ss} = 0.01$ and $e_{ss} = 1$, respectively.

$$C_1(s) = \frac{6.9978(s + 511)(s + 88.92)}{(s + 2355)(s + 1.946)} \tag{17}$$

$$C_2(s) = \frac{4.914(s + 511)(s + 250.7)}{(s + 1967)(s + 231.8)} \tag{18}$$

It can be seen that each of these controllers is of second order and is in the form of a lead-lag compensator.

6. Fuzzy logic controller design

A fuzzy logic controller (FLC) consists of four elements. These are a fuzzification interface, a rule base, an inference mechanism, and a defuzzification interface (Passino & Yurkovich, 1998). A FLC has to be designed for each of the four channels of the MBC500 magnetic system. The design of the FLC for channel x_2 is described in detail in this section. The design of the remaining FLCs will follow the same procedure. The FLC designed for the MBC500 magnetic bearing system in this section has two inputs and one output. The "Error" and "Rate of Change of Error" variables derived from the output from the MBC500 on-board hall-effect sensor will be used as the inputs. A voltage for controlling the current amplifiers on the MBC500 magnetic bearing system will be produced as the output. The shaft's schematic (top view) showing the electromagnets and the Hall-effect sensors is provided in Figure 6.

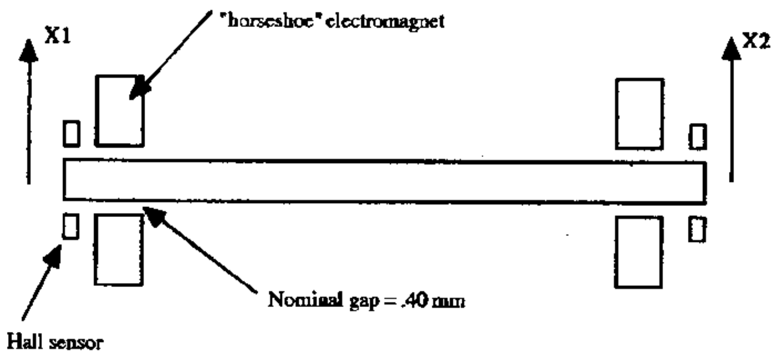

Fig. 6. Shaft schematic showing electromagnets and Hall-effect sensors (Magnetic Moments, 1995)

Figure 7 shows the single channel block diagram of the magnetic bearing system with the proposed FLC. A PD-Like FLC was designed to improve system damping as closed-loop stability is the major concern of the magnetic bearing system. As the MBC500 is a small magnetic bearing system, it has extremely fast dynamic responses which include the vibrations at *770 Hz* and *2050 Hz*. Therefore, a sampling frequency of *20kHz* (or a sample period of 50 microseconds) was deemed necessary.

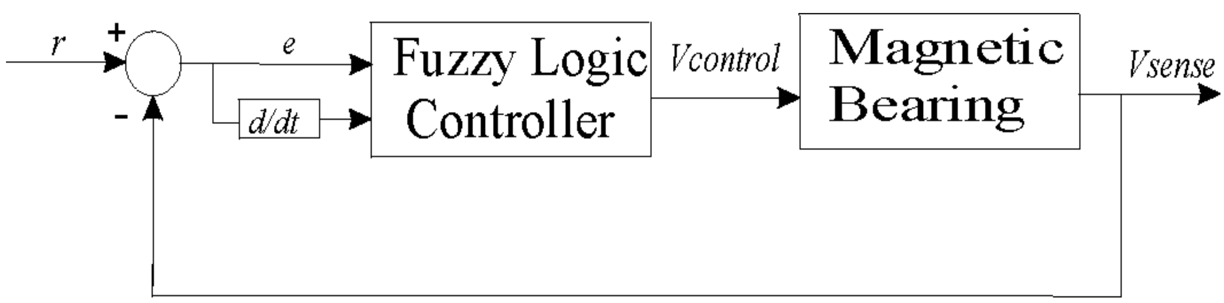

Fig. 7. FLC for MBC500 magnetic bearing system

Figure 8 illustrates the horizontal orientation (top view) of the MBC500 magnetic bearing shaft with the corresponding centre reference line, and its output and input at the right hand side (that is, channel 2).

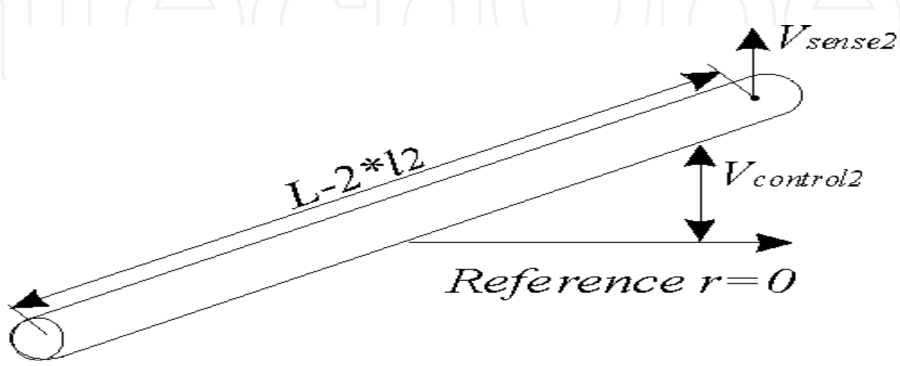

Fig. 8. MBC500 magnetic bearing control at the right hand side for channel x_2

The displacement output x_2 is sensed by the Hall-effect sensor as the voltage V_{sense2}. Hence the error signal is defined for channel x_2 as:

$$e(t) = r(t) - V_{sense2}(t)$$

For the magnetic bearing stabilization problem, the reference input is *r(t) = 0*. As a result,

$$e(t) = -V_{sense2}(t)$$

and

$$\frac{d}{dt}e(t) = -\frac{d}{dt}V_{sense2}(t)$$

The linguistic variables which describe the FLC inputs and outputs are:

"Error" denotes *e(t)*
"Rate of change of error" denotes $\frac{d}{dt}e(t)$
"Control voltage" denotes $V_{control2}$

The above linguistic variables "error", "rate of change of error," and "control voltage" will take on the following linguistic values:

"NB" = Negative Big
"NS" = Negative Small
"ZO" = Zero
"PS" = Positive Small
"PB" = Positive Big

Drawing on the design concept of the FLC for an inverted pendulum on a cart described in (Passino & Yurkovich, 1998) the following statements can be developed to illustrate the linguistic quantification of the different conditions of the magnetic bearing:

- The statement "error is PB" represents the situation where the magnetic bearing shaft is significantly below the reference line.
- The statement "error is NS" represents the situation where the magnetic bearing shaft is just slightly above the reference line. However, it is neither too close to the centre reference position to be quantified as "ZO" nor it is too far away to be quantified as "NB".
- The statement "error is ZO" represents the situation where the magnetic bearing shaft is sufficiently close to the centre reference position. As a linguistic quantification is not precise, any value of the error around e(t) = 0 will be accepted as "ZO" as long as this can be considered as a better quantification than "PS" or "NS".
- The statement "error is PB and rate of change of error is PS" represents the situation where the magnetic bearing shaft is significantly below the centre reference line and, since $\frac{d}{dt}V_{sense2} < 0$, the magnetic bearing shaft is moving slowly away from the centre position.

- The statement "error is NS and rate of change of error is PS" represents the situation where the magnetic bearing shaft is slightly above the centre reference line and, since $\frac{d}{dt}V_{sense2} < 0$, the magnetic bearing shaft is moving slowly towards the centre position.

We shall use the above linguistic quantification to specify a set of rules or a rule-base. The following three situations will demonstrate how the rule-base is developed.

1. If error is NB and rate of change of error is NB Then force is NB.

Figure 9 shows that the magnetic bearing shaft at the right end is significantly above the centre reference line and is moving away from it quickly. Therefore, it is clear that a strong negative force should be applied so that the shaft will move to the centre reference position.

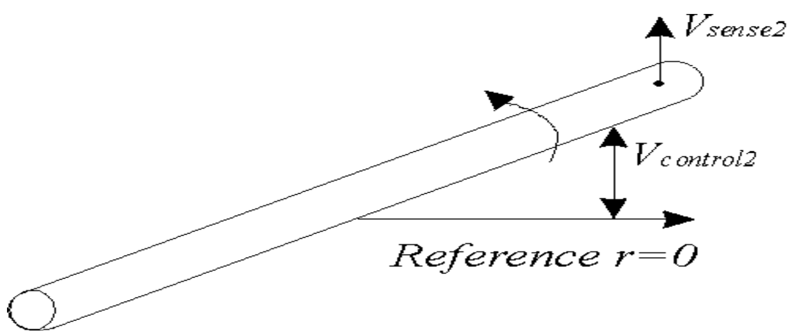

Fig. 9. Magnetic bearing shaft at the right end with a positive displacement

2. If error is ZO and rate of change of error is PS Then force is PS.

Figure 10 shows that the bearing shaft at the right end has a displacement of nearly zero from the centre reference position (a linguistic quantification of zero does not imply that e(t)=0 exactly) and is moving away (downwards) from the centre reference line. Therefore, a small positive force should be applied to counteract the movement so that it will move towards the centre reference position.

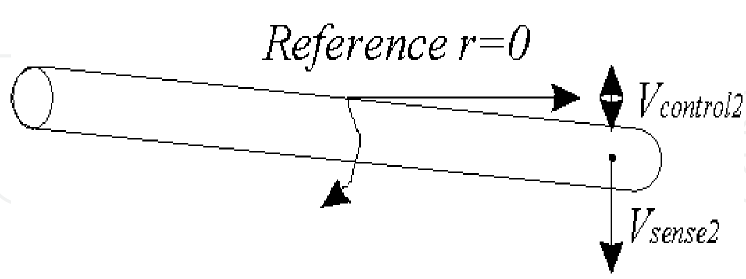

Fig. 10. Magnetic bearing shaft at the right end with zero displacement

3. If error is PB and rate of change of error is NS Then force is PS.

Figure 11 shows that the bearing shaft at the right end is far below the centre reference line and is moving towards the centre reference position. Therefore, a small positive force should be applied to assist the movement. However, it should not be too large a force since the bearing shaft at the right end is already moving in the correct direction.

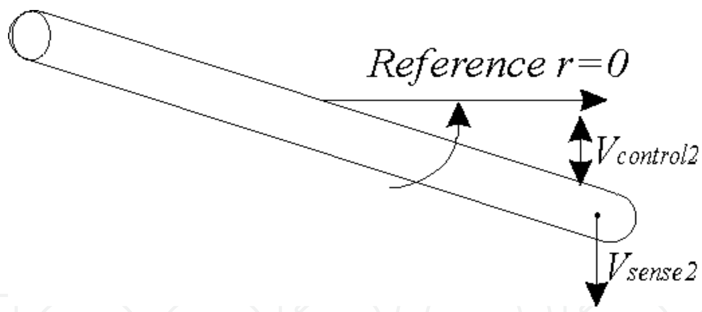

Fig. 11. Magnetic bearing shaft at the right end with a negative displacement

Following a similar analysis, the rules of the FLC for controlling the magnetic bearing shaft can be developed. For the FLC with two inputs and five linguistic values for each input, there are 5^2=25 possible rules with all combination for the inputs. A set of possible linguistic output values are NB, NS, ZO, PS and PB. The tabular representation of the FLC rule base (with 25 rules) of the magnetic bearing fuzzy control system is shown in Table 1.

"control voltage" V		"rate of change of error" $\dot{e}$				
		NB	NS	ZO	PS	PB
"error" e	NB	NB	NB	NB	NS	ZO
	NS	NB	NB	NS	ZO	PS
	ZO	NB	NS	ZO	PS	PM
	PS	NS	ZO	PS	PB	PB
	PB	ZO	PS	PB	PB	PB

Table 1. Rule table with 25 rules

The membership functions to be employed are of the triangular type where, for any given input, there are only two membership functions premises to be calculated. This is in contrast to Gaussian membership functions where each requires more than two premise outputs and can generate a large amount of calculations per final output. The triangular membership functions used is shown in Figure 12:

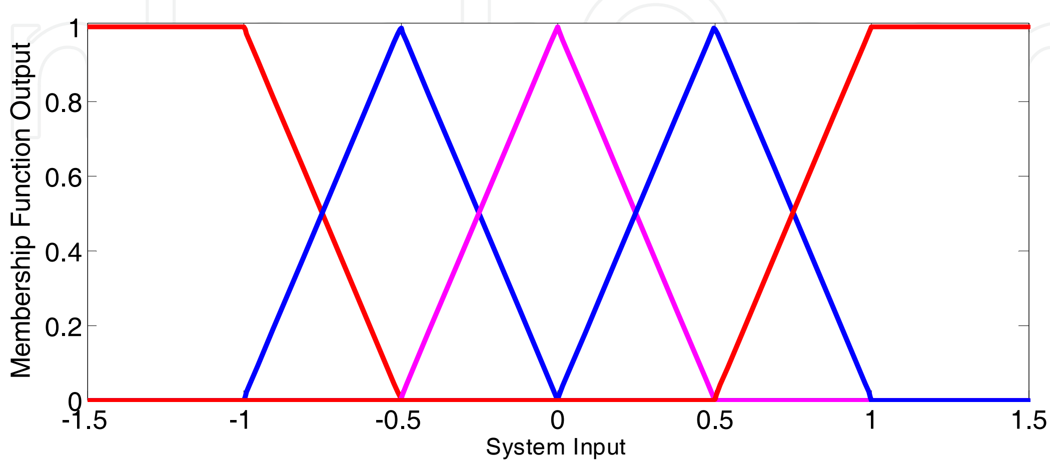

Fig. 12. Triangular Membership Function

The membership functions shown in Figure 12 represent the linguistic values NB, NS, ZO, PS, PB (from left to right).

The inference method used for the designed FLC is Takagi-Sugeno Method (Passino & Yurkovich, 1998) and the centre average method is used in the defuzzification process (Passino & Yurkovich, 1998).

7. Simulation Results

By using the designed conventional controller $C_{lead}(s)$, the controllers $C(s)$, $C_1(s)$, *and* $C_2(s)$ designed via the analytical interpolation method, and the FLC designed in Section 6, the closed-loop responses to a unit-step reference (applied at t = 0) and a unit-step disturbance (applied at t = 0.05 seconds) and the corresponding control signals are shown in Figure 13 and Figure 14, respectively. In all of the simulations, the full 8th-order plant model described by equation (1) was employed.

It is important to note that the DC gain designed into each of $C(s)$ and $C_1(s)$ via interpolation has forced the steady-state error to be the small value specified. It is also important to note that while the closed-loop unit step responses with $C_{lead}(s)$ and $C_2(s)$ have comparable steady-state errors (approximately -1), the closed-loop unit-step response with $C_2(s)$ has a much better transient responses than that with $C_{lead}(s)$. (Similar comment also applies to their disturbance rejection behaviours). Furthermore, it is apparent that trade-off between steady-state error and transient response can be easily achieved with controllers designed via the interpolation approach presented in Section 5.

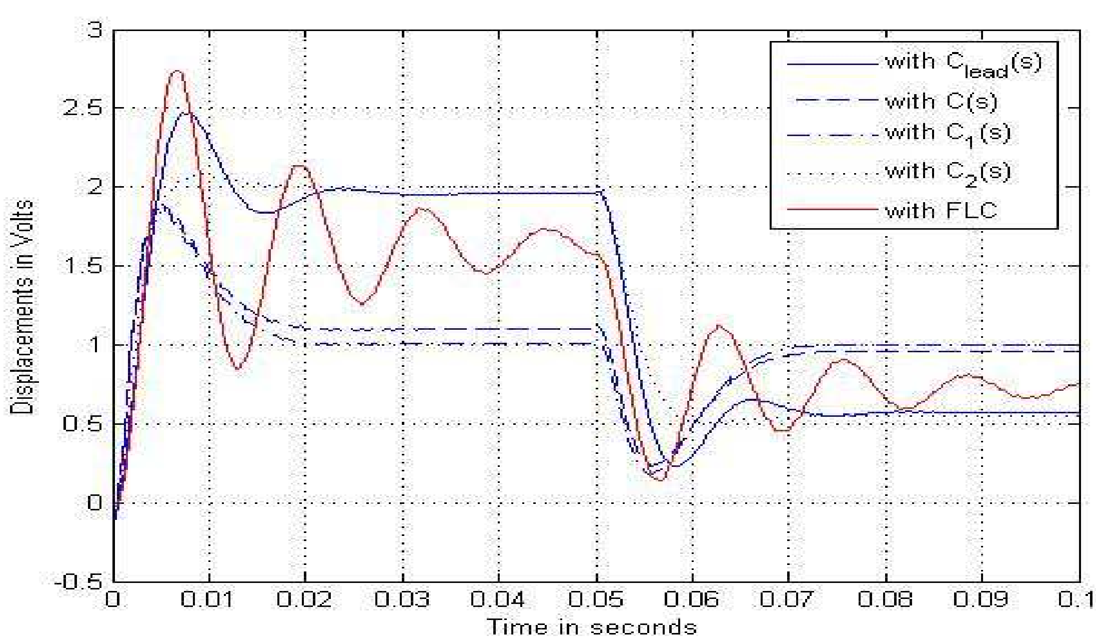

Fig. 13. Closed-loop responses of the MBC500 magnetic bearing system to step reference and step disturbance with controllers $C_{lead}(s)$, $C(s)$, $C_1(s)$, *and* $C_2(s)$, and the designed FLC.

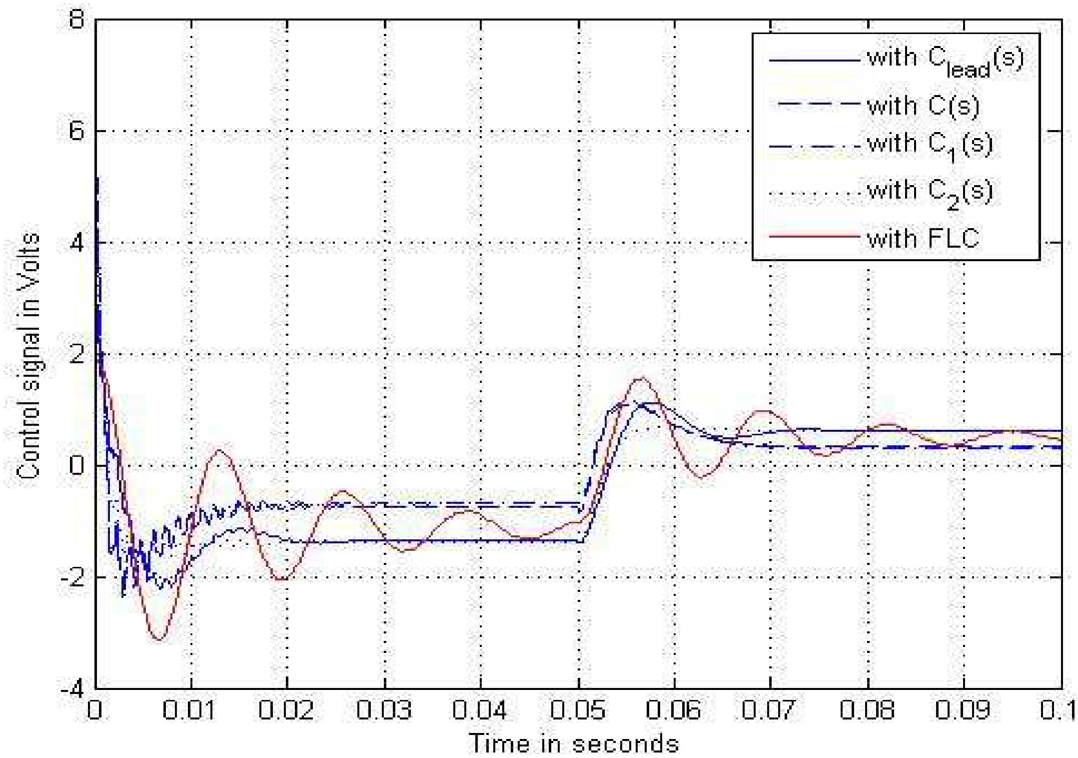

Fig. 14. Closed-loop responses of the MBC500 magnetic bearing system to step reference and step disturbance with controllers $C_{lead}(s)$, $C(s)$, $C_1(s)$, *and* $C_2(s)$, and the designed FLC.

It can also be observed that the closed-loop unit step responses obtained with the designed FLC exhibits more oscillations. However, it must be pointed out that two elliptic notch filters to notch out the resonant modes of the MBC500 magnetic bearing system located at approximately 770 Hz and 2050 Hz were employed with both the conventional controller and the controllers designed via analytical interpolation approach to ensure system stability. For the designed FLC, system stability is achieved without the need of using the two notch filters.

From Figures 13 and 14 it can be seen that the system is stable and reasonably well compensated by all the controllers designed. These controllers are now ready to be coded in C language and implemented in real-time.

8. Implementation of the designed Controllers

In order to implement the designed notch filters and controllers, a dSPACE DS1102 processor board, MatLab, Simulink and dSPACE Control Desk are used. The controllers $C_{lead}(s)$ and $C_2(s)$ are represented as a block diagram via a Simulink file, which allows it to be connected to the ADC and the DAC of the DS1102 processor board. The DS1102 DSP board can then execute the designed controllers (discretized via the bilinear-transformation method) through MatLab's Real-Time Workshop.

In this magnetic bearing system, for the model based controllers the notch filters act to provide damping to the rotor resonances near 770 Hz and 2050 Hz. The sampling frequency was originally chosen to be 25 kHz to avoid aliasing of frequencies within the normal operating frequency range (Shi & Revell, 2002). The maximum possible sampling frequency with the FLC was 20 kHz (Shi & Lee, 2008) due to the longer C code implementation requirement of the FLC. In order to have a fair comparison of the system responses, the sampling frequencies of the model based controllers and the FLC were both set at 20kHz.

In the following, we shall present and compare the experimental results. Preliminary observation has revealed that the performance of the controller $C_2(s)$ designed via analytical interpolation approach is most similar to $C_{lead}(s)$ and the FLC. As a result, the performance of $C_2(s)$ will be investigated in detail in the implementation. We shall first compare the results for the model based controllers and the FLC under steady-state conditions. We shall then compare the disturbance rejection results of the closed-loop system employing each of these controllers.

8.1 Comparison of Steady-state Responses

Figure 15 shows the steady-state responses of the magnetic bearing system when it is under the control of the model based controllers and the FLC, respectively.

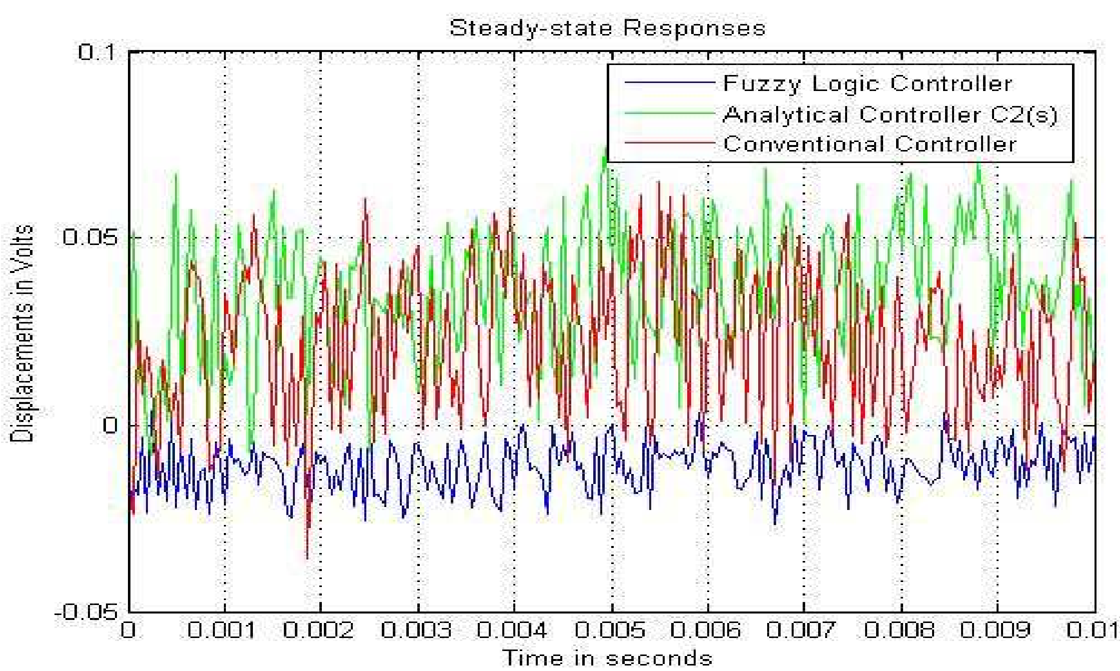

Fig. 15. Steady-state responses with the model based controllers and FLC

It can be seen in Figure 15 that the displacement sensor outputs were noisy when the magnetic bearing system is controlled by either the model based controller or the FLC. However, the response with the FLC has a smaller steady-state error (i.e. closer to zero). Investigation via analysis and simulation has revealed that the source of the noise in the outputs was measurement noise.

8.2 Comparison of Step and Disturbance Rejection Responses

Figure 16 and Figure 17 show the displacement sensor output and the controller output, respectively, when a step disturbance of 0.05V is applied to the channel 1 input of the magnetic bearing system when it is controlled with the model based conventional controller $C_{lead}(s)$. Note that the displacement sensor output is multiplied by a factor of 10 when it is transmitted through the DAC.

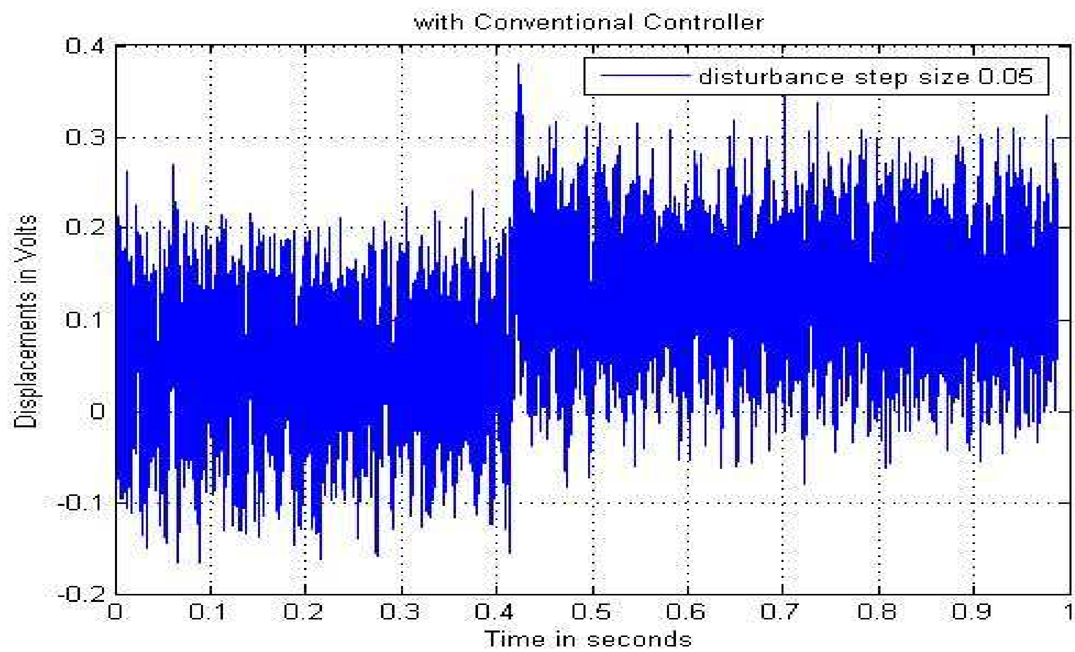

Fig. 16. Displacement output of the MBC500 magnetic bearing system with the model based controller $C_{lead}(s)$.

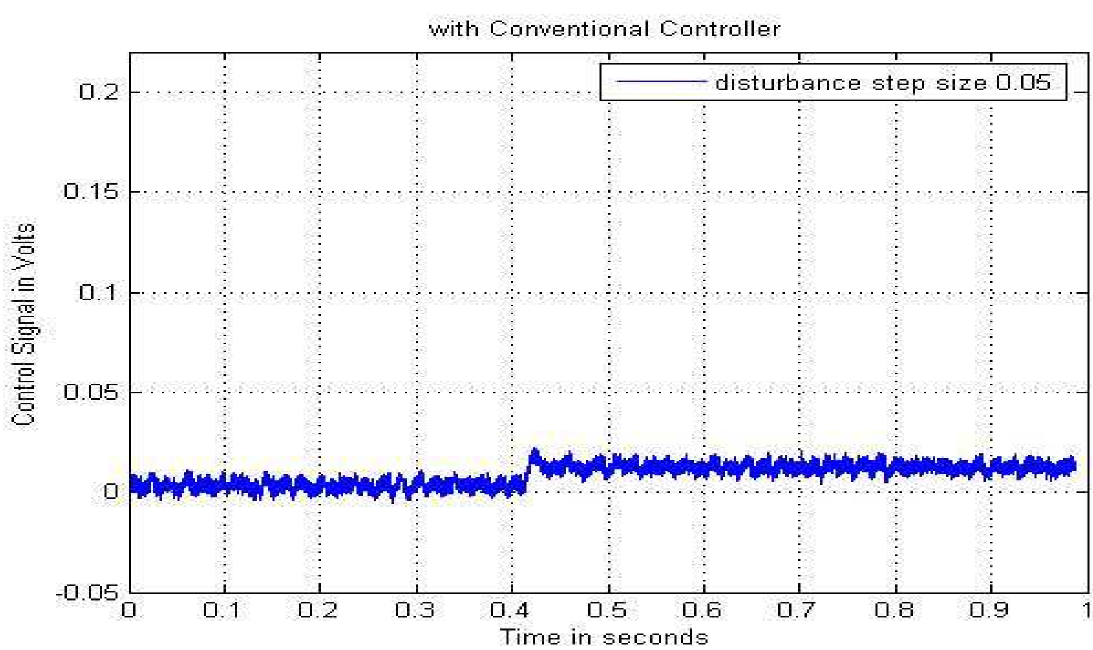

Fig. 17. Control signal of the MBC500 magnetic bearing system with the model based controller $C_{lead}(s)$.

Figure 18 and Figure 19 show the displacement sensor output and the controller output, respectively, when a step change in disturbance of *0.1V* is applied to the channel 1 input of the magnetic bearing system when it is controlled with the model based controller.

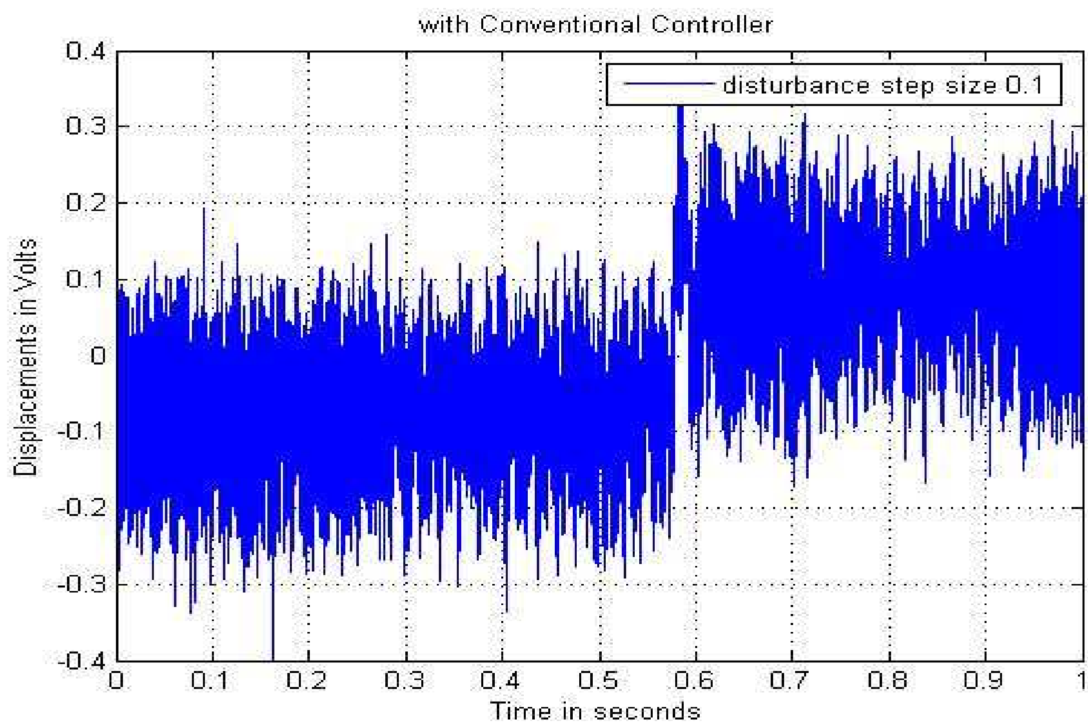

Fig. 18. Step response of the MBC500 magnetic bearing system with the model based controller $C_{lead}(s)$.

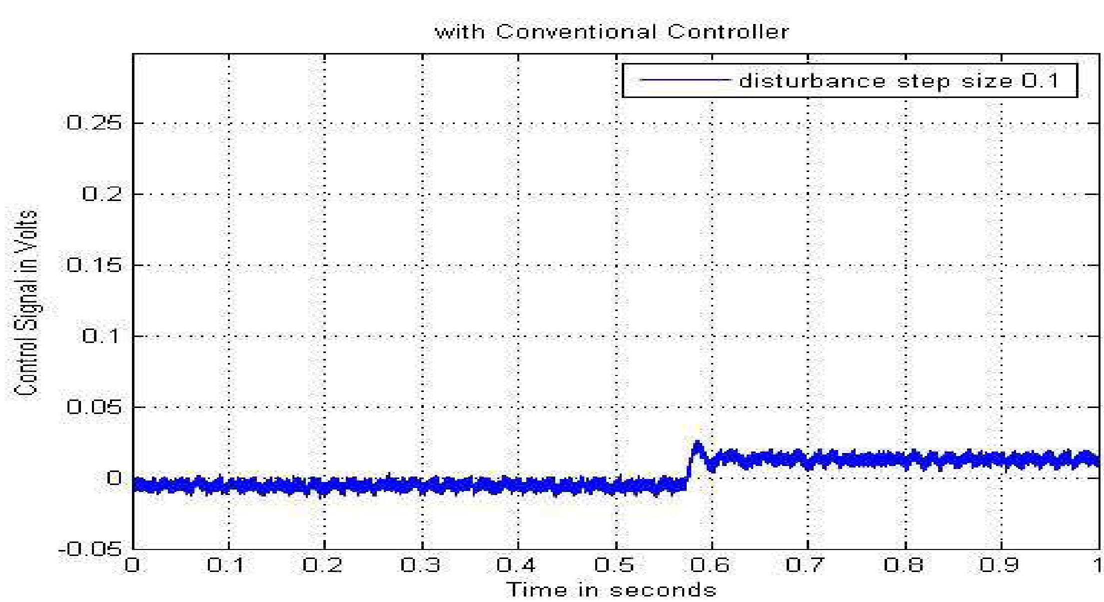

Fig. 19. Control signal of the MBC500 magnetic bearing system with the model based controller $C_{lead}(s)$.

Figure 20 and Figure 21 show the displacement sensor output and the controller output, respectively, when a step change in disturbance of *0.5V* is applied to the channel *1* input of the magnetic bearing system when it is controlled with the conventional controller $C_{lead}(s)$.

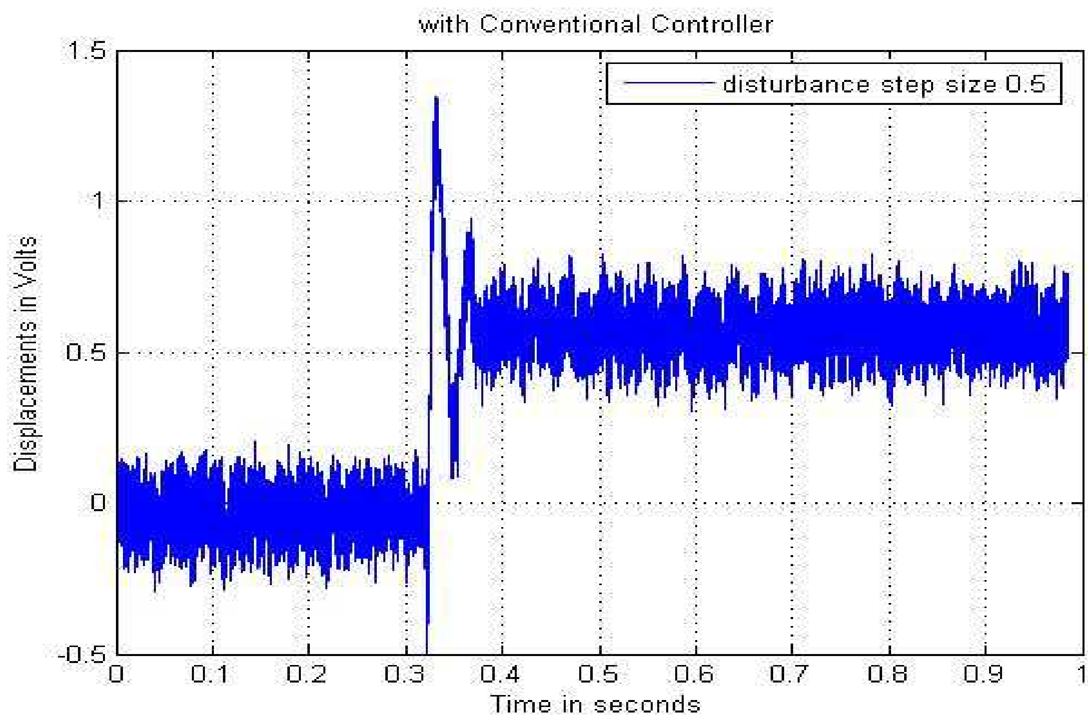

Fig. 20. Step response of the MBC500 magnetic bearing system with the model based controller $C_{lead}(s)$.

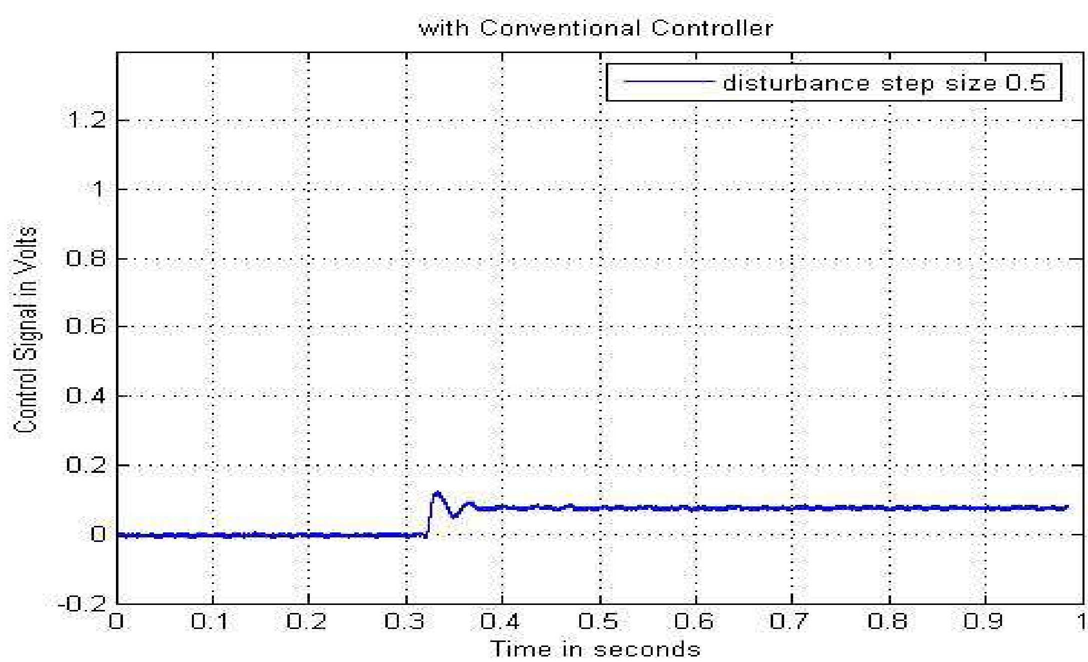

Fig. 21. Control signal of the MBC500 magnetic bearing system with the model based controller $C_{lead}(s)$.

It can be seen from the above figures that the magnetic bearing system remain stable under the control of the model based conventional controller when a step change in disturbance of is applied to its channel *1* input. Similar results were also obtained from other channels.

Figure 22 and Figure 23 show the displacement sensor output and the controller output, respectively, when a step change in disturbance of *0.05V* is applied to the channel *1* input of the magnetic bearing system when it is controlled with the analytical controller $C_2(s)$.

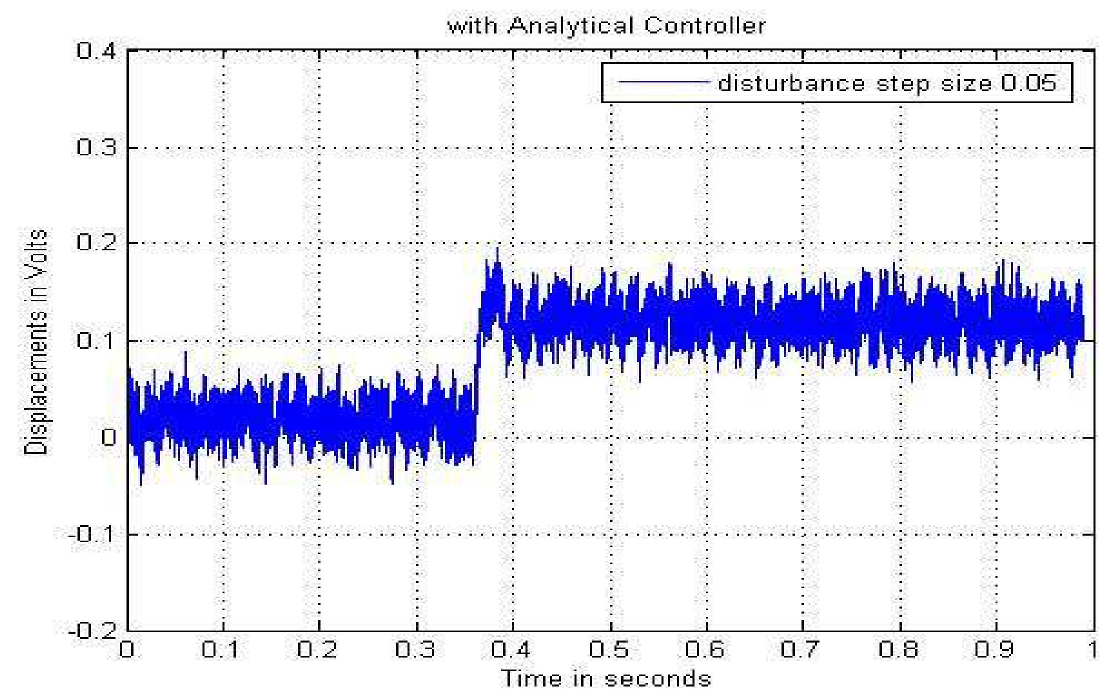

Fig. 22. Displacement output of the MBC500 magnetic bearing system with the analytical controller $C_2(s)$.

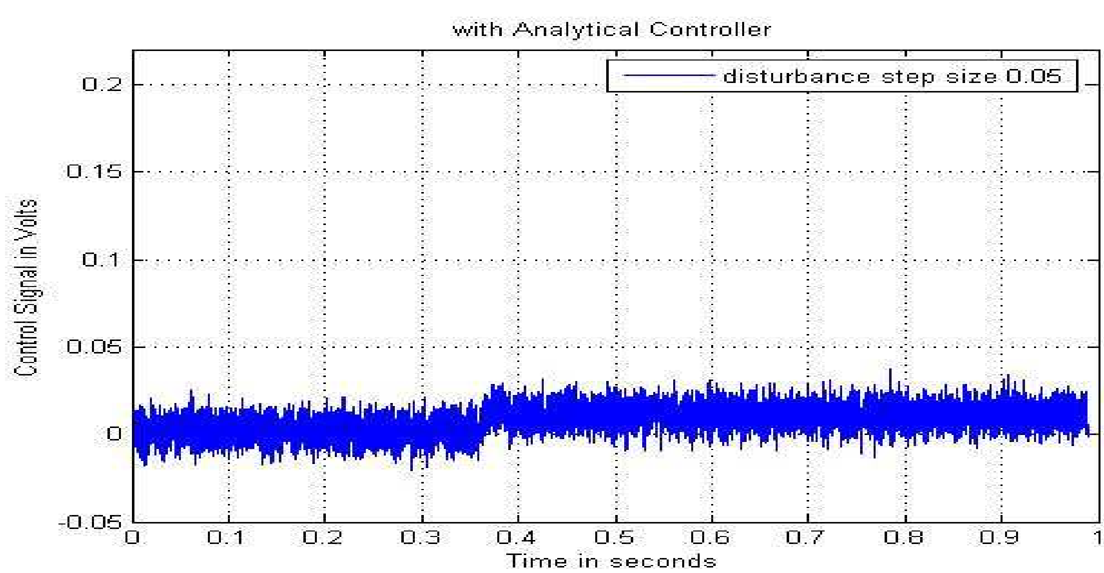

Fig. 23. Control signal of the MBC500 magnetic bearing system with the analytical controller $C_2(s)$.

Figure 24 and Figure 25 show the displacement sensor output and the controller output, respectively, when a step change in disturbance of *0.1V* is applied to the channel *1* input of the magnetic bearing system when it is controlled with the analytical controller $C_2(s)$.

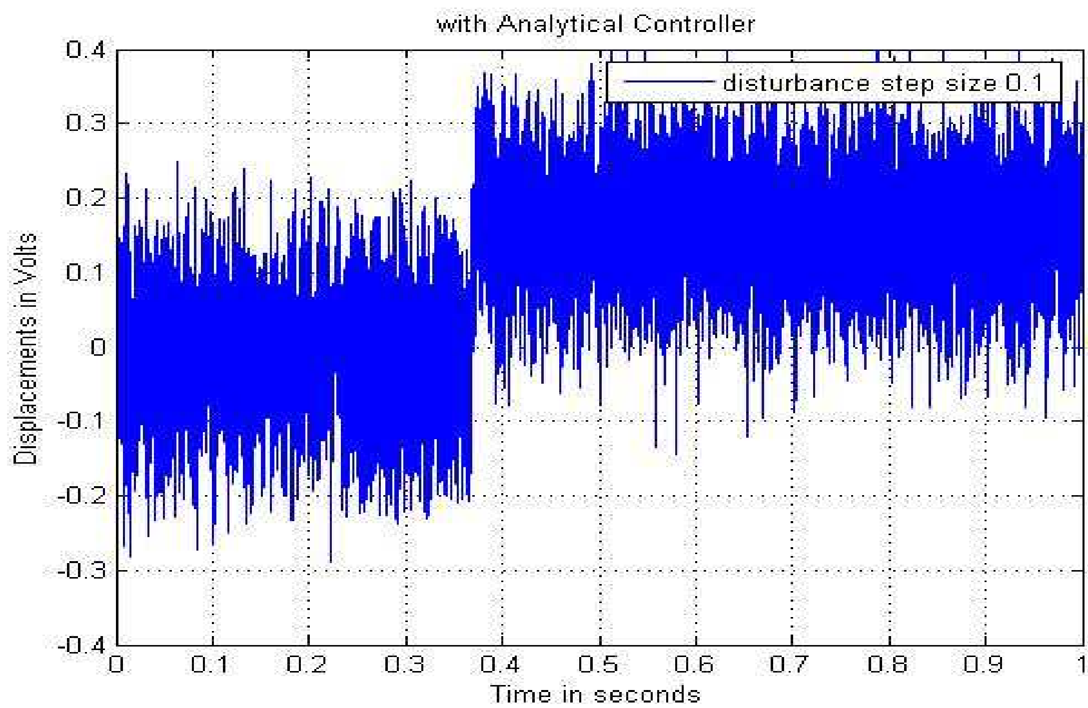

Fig. 24. Displacement output of the MBC500 magnetic bearing system with the analytical controller $C_2(s)$.

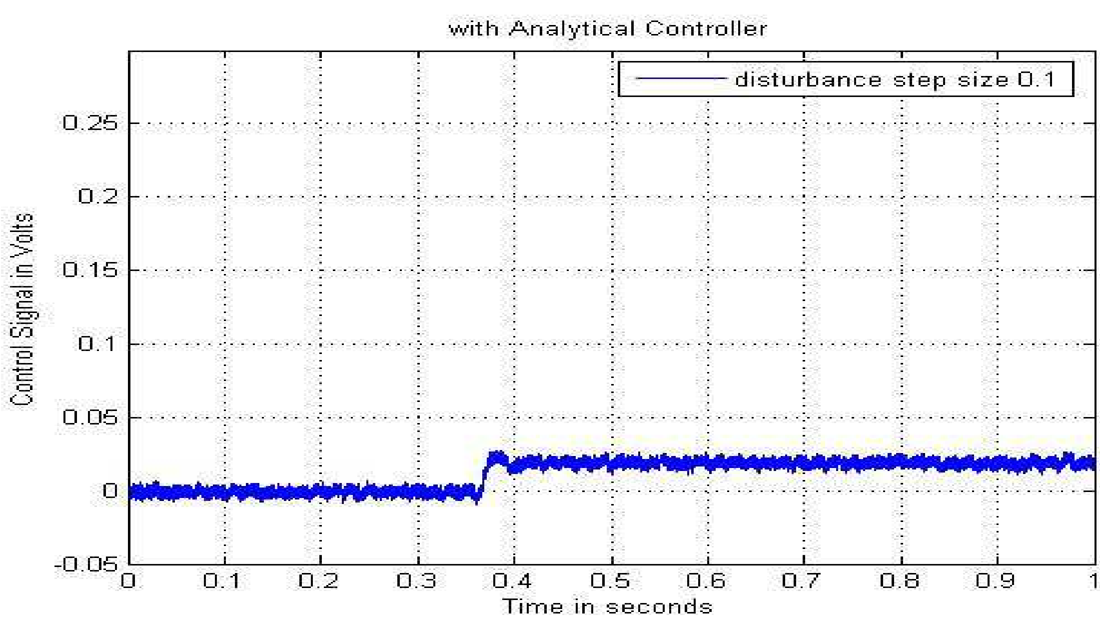

Fig. 25. Control signal of the MBC500 magnetic bearing system with the analytical controller $C_2(s)$.

Figure 26 and Figure 27 show the displacement sensor output and the controller output, respectively, when a step change in disturbance of *0.5V* is applied to the channel *1* input of the magnetic bearing system when it is controlled with the analytical controller $C_2(s)$.

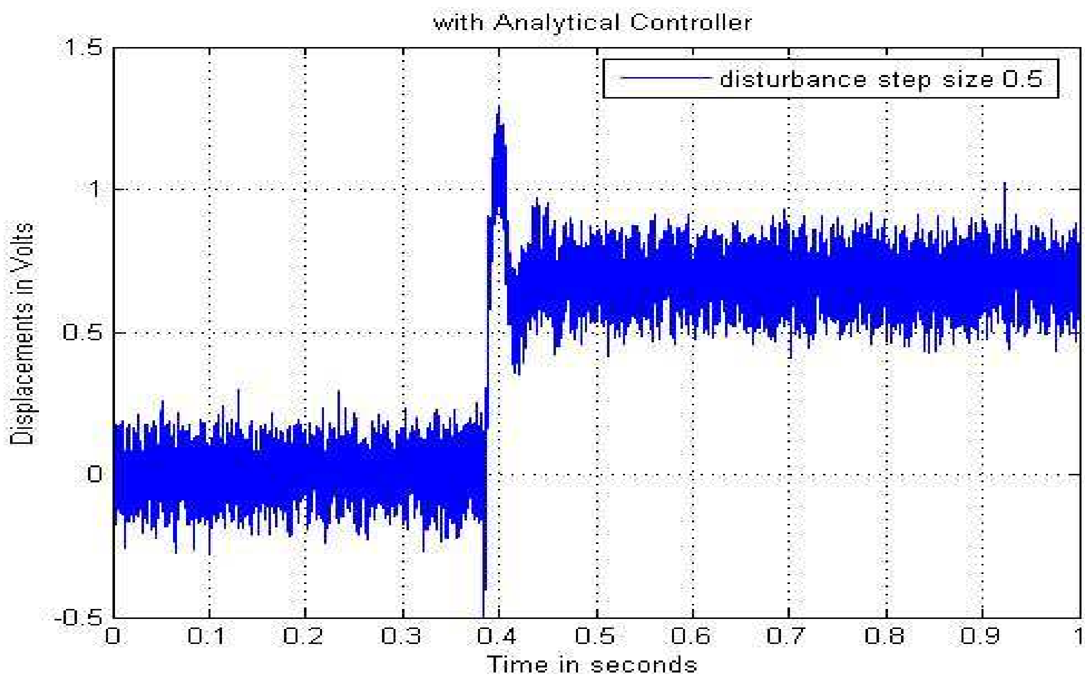

Fig. 26. Displacement output of the MBC500 magnetic bearing system with the analytical controller $C_2(s)$.

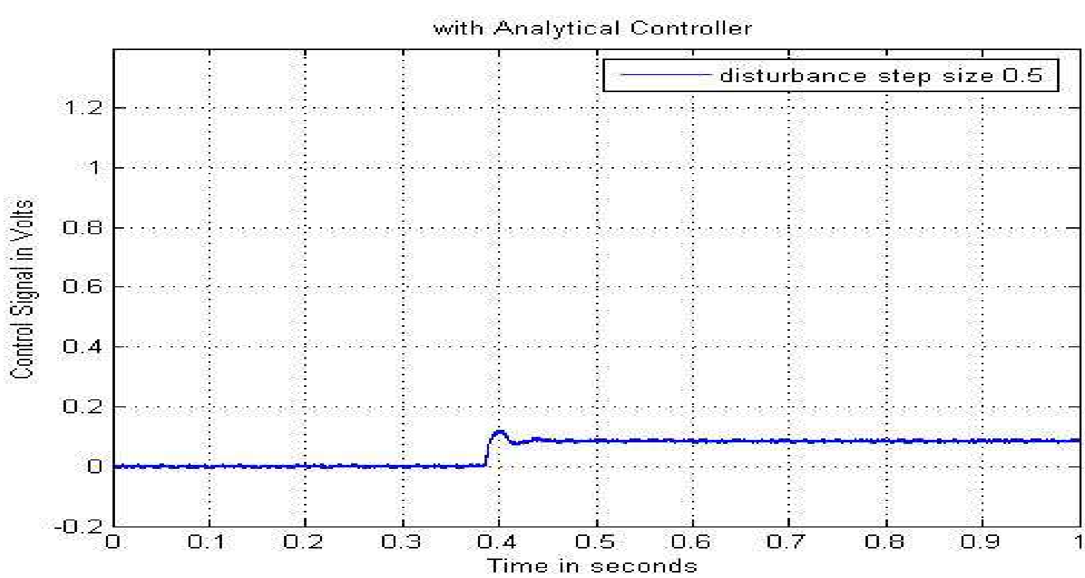

Fig. 27. Control signal of the MBC500 magnetic bearing system with the analytical controller $C_2(s)$.

Figure 28 and Figure 29 show the displacement sensor output voltage and the controller output voltage, respectively, when a step of *0.05V* is applied to channel *1* of the magnetic bearing system, when it is controlled with the FLC.

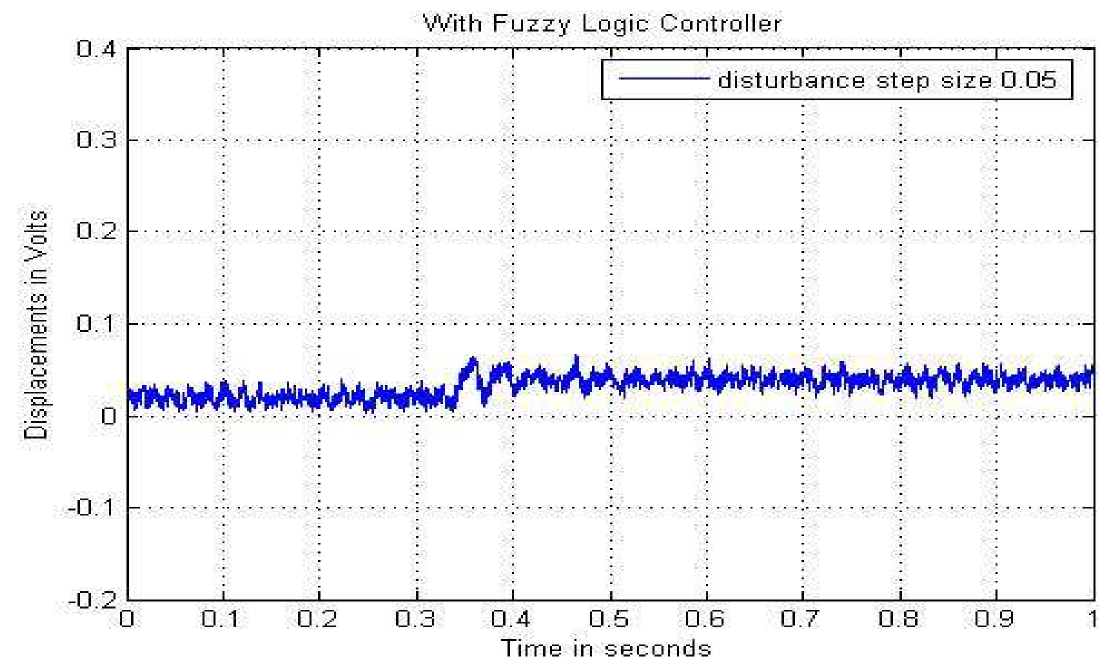

Fig. 28. Step response of the MBC500 magnetic bearing system with the FLC.

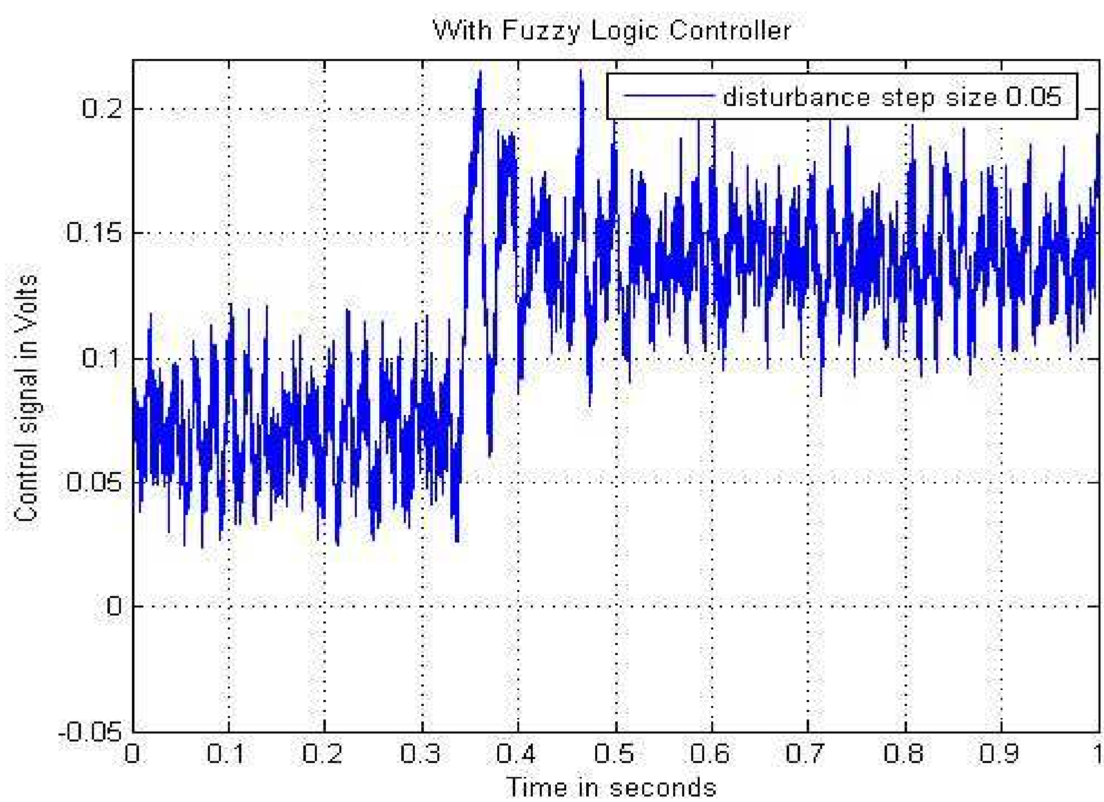

Fig. 29. Control signal of the MBC500 magnetic bearing system with the FLC.

Figure 30 and Figure 31 show the displacement sensor output voltage and the controller output voltage, respectively, when a step of *0.1V* is applied to channel *1* of the magnetic bearing system, when it is controlled with the FLC.

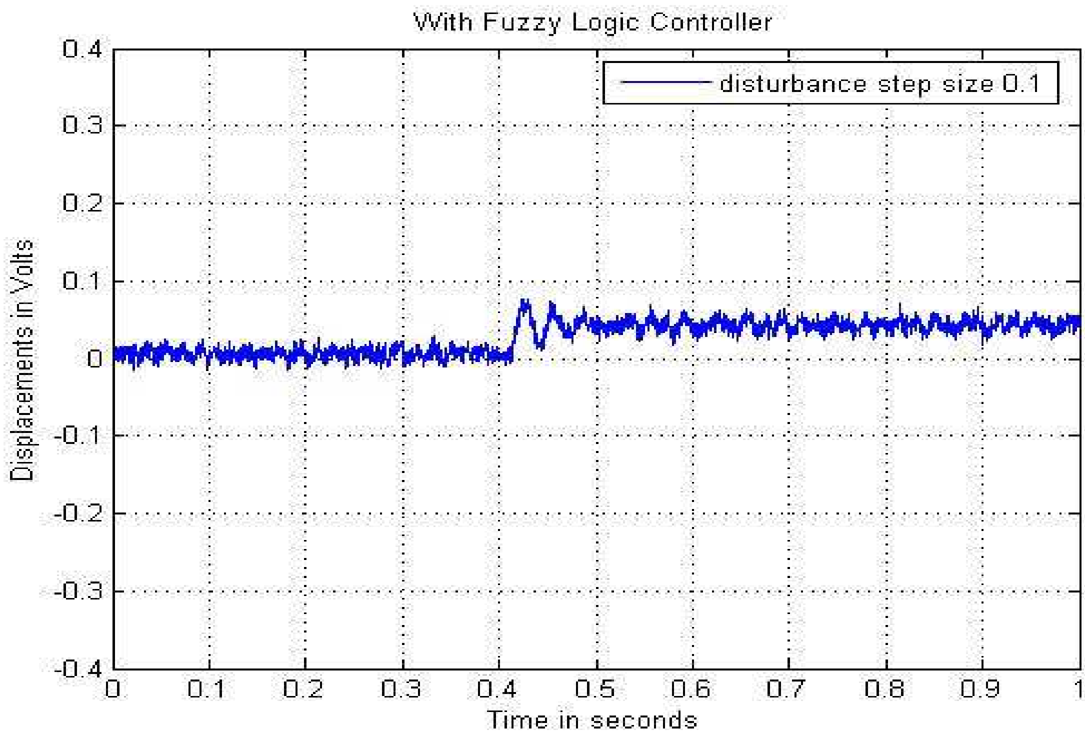

Fig. 30. Step response of the MBC500 magnetic bearing system with the FLC.

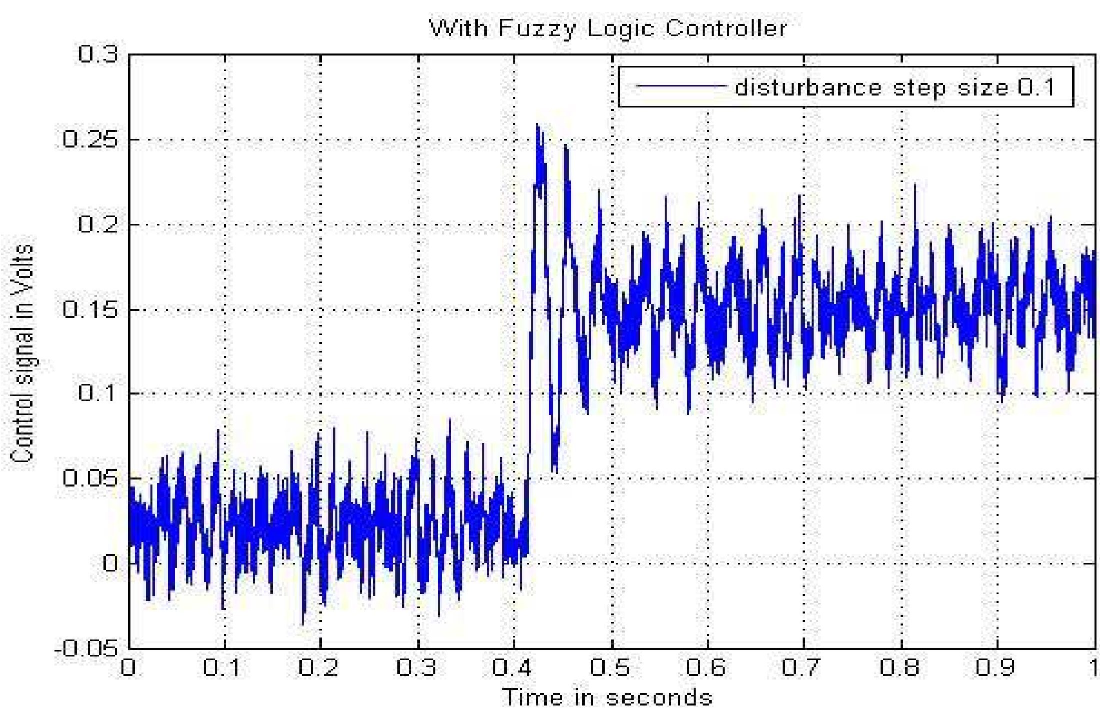

Fig. 31. Control signal of the MBC500 magnetic bearing system with the FLC.

Figure 32 and Figure 33 show the displacement sensor output and the controller output, respectively, when a step change in disturbance of *0.5V* is applied to the channel *1* input of the magnetic bearing system when it is controlled with the FLC.

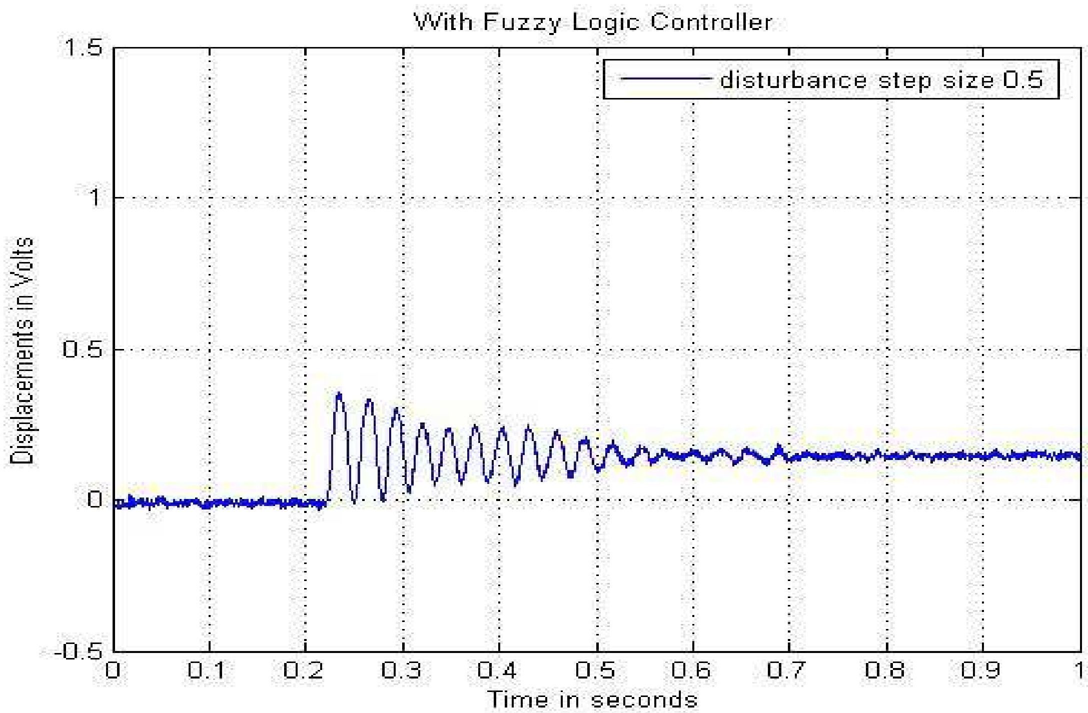

Fig. 32. Step response of the MBC500 magnetic bearing system with the FLC.

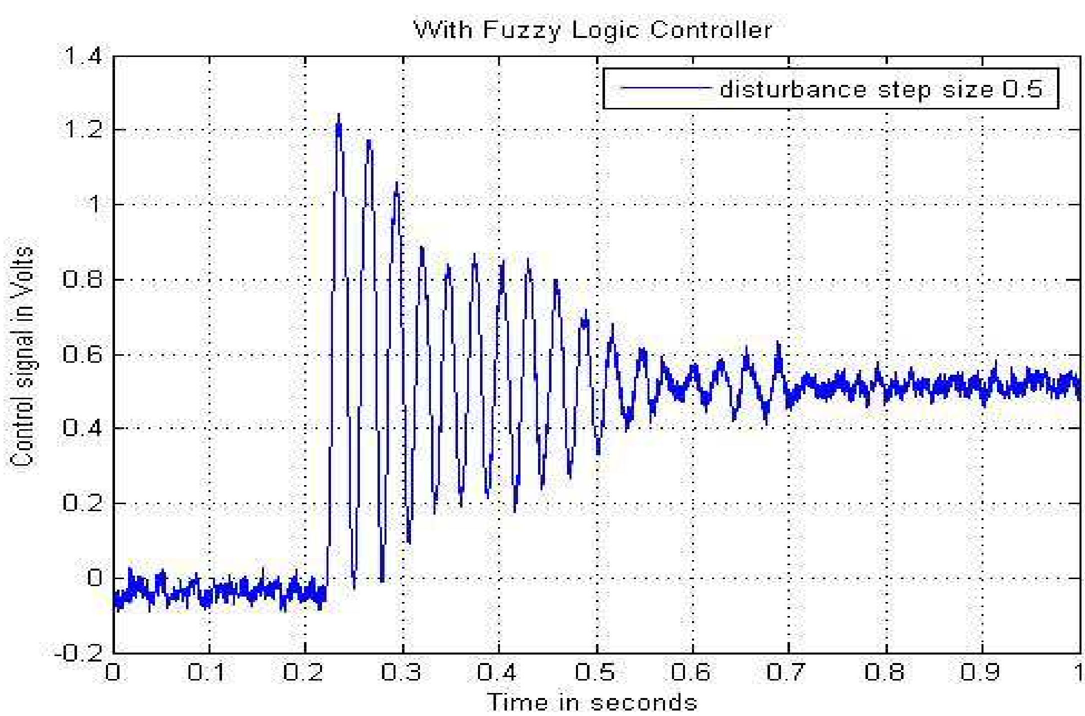

Fig. 33. Control signal of the MBC500 magnetic bearing system with the FLC.

The FLC was tested extensively to ensure that it can operate in a wide range of conditions. These include testing its tolerance to the resonances of the MBC500 system by tapping the rotor with screwdrivers. The system remained stable throughout the whole regime of testing. The MBC500 magnetic bearing system has four different channels; three of the channels were successfully stabilized with the single FLC designed without any modifications or further adjustments. For the channel that failed to be robustly stabilized, the difficulty could be attributed to the strong resonances in that particular channel which have very large magnitude. After some tuning to the input and output scaling values of the FLC, robust stabilization was also achieved for this difficult channel.

Comparing Figures 16 and 22, 18 and 24, 20 and 26, it can be seen that the system step responses with the controller designed via analytical interpolation approach exhibit smaller overshoot and shorter settling time with similar control effort as shown in Figures 17 and 23, 19 and 25, 21 and 27. The step and step disturbance rejection responses with the designed FLC exhibit smaller steady-state error and overshoot as shown in Figures 28, 30 and 32 with much bigger control signal displayed in Figures 29, 31 and 33. However, it must be pointed out that the system stability is achieved with the designed FLC without using the two notch filters to eliminate the unwanted resonant modes.

9. Conclusion and future work

In this chapter, the controller structure and performance of a conventional controller and an analytical feedback controller have been compared with those of a fuzzy logic controller (FLC) when they are applied to the MBC500 magnetic bearing system stabilization problem.

The conventional and the analytical feedback controller were designed on the basis of a reduced order model obtained from an identified 8^{th}-order model of the MBC500 magnetic bearing system. Since there are resonant modes that can threaten the stability of the closed-loop system, notch filters were employed to help secure stability.

The FLC uses error and rate of change of error in the position of the rotor as inputs and produces an output voltage to control the current of the amplifier in the magnetic bearing system. Since a model is not required in this approach, this greatly simplified the design process. In addition, the FLC can stabilize the magnetic bearing system without the use of any notch filters. Despite the simplicity of FLC, experimental results have shown that it produces less steady-state error and has less overshoot than its model based counterpart.

While the model based controllers are linear systems, it is not a surprise that their stability condition depends on the level of the disturbance. This is because the magnetic bearing system is a nonlinear system. However, although the FLC exhibits some of the common characteristics of high authority linear controllers (small steady-state error and amplification of measurement noise), it does not have the low stability robustness property usually associated with such high gain controllers that we would have expected.

Future work will include finding some explanations for the above unusual observation on FLC. We believe the understanding achieved through attempting to address the above issue would lead to better controller design methods for active magnetic bearing systems.

10. References

Williams, R.D, Keith, F.J., and Allaire, P.E. (1990). Digital Control of Active Magnetic Bearing, *IEEE trans. on Indus. Electr*. Vol. 37, No. 1, pp. 19-27, February 1990.

Lee, K.C, Jeong, Y.H., Koo, D.H., and Ahn, H. (2006) Development of a Radial Active Magnetic Bearing for High Speed Turbo-machinery Motors, *Proceedings of the 2006 SICE-ICASE International Joint Conference*, 1543-1548, 18-21 October, 2006.

Bleuler, H., Gahler, C., Herzog, R., Larsonneur, R., Mizuno, T., Siegwart, R. (1994) Application of Digital Signal Processors for Industrial Magnetic Bearings, *IEEE Trans. on Control System Technology,* Vol. 2, No. 4, pp. 280-289, December 1994.

Magnetic Moments (1995), LLC, *MBC 500 Magnetic Bearing System Operating Instructions*, December, 1995.

Shi, J. and Revell, J. (2002) System Identification and Reengineering Controllers for a Magnetic Bearing System, *Proceedings of the IEEE Region 10 Technical Conference on Computer, Communications, Control and Power Engineering*, Beijing, China, pp.1591-1594, 28-31 October, 2002.

Dorato, P. (1999) *Analytic Feedback System Design: An Interpolation Approach*, Brooks/Cole, Thomson Learning, 1999.

Dorato, P., Park, H.B., and Li, Y. (1989) An Algorithm for Interpolation with Units in $H\infty$, with Applications to Feedback Stabilization, *Automatica*, Vol. 25, pp.427-430, 1989.

Shi, J., and Lee, W.S. (2009) Analytical Feedback Design via Interpolation Approach for the Strong Stabilization of a Magnetic Bearing System, *Proceedings of the 2009 Chinese Control and Decision Conference (CCDC2009)*, Guilin, China, 17-19 June, 2009, pp. 280-285.

Shi, J., Lee, W.S., and Vrettakis, P. (2008) Fuzzy Logic Control of a Magnetic Bearing System, *Proceedings of the 20th Chinese Control and Decision Conference(2008 CCDC),* Yantai, China, 1-6, 2-4 July, 2008.

Shi, J., and Lee, W.S. (2009) An Experimental Comparison of a Model Based Controller and a Fuzzy Logic Controller for Magnetic Bearing System Stabilization, *Proceedings of the 7th IEEE International Conference on Control & Automation (**ICCA'09**)*, Christchurch, New Zealand, 9-11 December, 2009, pp. 379-384.

Habib, M.K., and Inayat-Hussain, J.I. (2003). Control of Dual Acting Magnetic Bearing Actuator System Using Fuzzy Logic, *Proceedings 2003 IEEE International Symposium on Computational Intelligence in Robotics and Automation*, Kobe, Japan, pp. 97-101, July 16-20, 2003.

Morse, N., Smith, R. and Paden, B. (1996) Magnetic Bearing System Identification, *MBC 500 Magnetic System Operating Instructions*, pp.1-14, May 29, 1996.

Van den Hof, P.M.J. and Schrama, R.J.P. (1993) "An indirect method for transfer function estimation from closed-loop data", Automatica, Volume 29, Issue 6, pp.1523-1527, 1993.

Freudenberg, J.S. and Looze, D.P. (1985), Right Half Plane Poles and Zeros and Design Tradeoffs in Feedback Systems, *IEEE Trans. Automat. Control,* 30, pp.555-565, 1985.

Dorato, P. (1999) *Analytic Feedback System Design: An Interpolation Approach*, Brooks/Cole, Thomson Learning, 1999.

Youla, D.C., Borgiorno J.J. Jr., and Lu, C.N. (1974) Single-loop feedback stabilization of linera multivariable dynamical plants, *Automatica*, Vol. 10, 159-173, 1974.

Passino, K.M. and Yurkovich, S. (1998) *Fuzzy Control*, Addison-Wesley Longman, Inc., 1998.

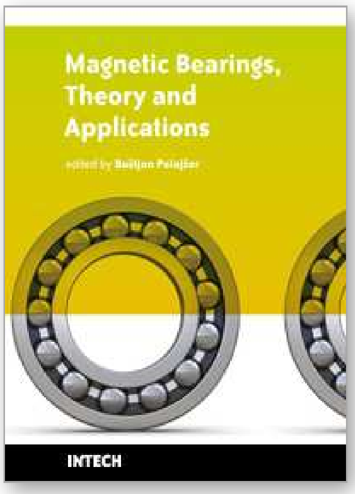

Magnetic Bearings, Theory and Applications
Edited by Bostjan Polajzer

ISBN 978-953-307-148-0
Hard cover, 132 pages
Publisher Sciyo
Published online 06, October, 2010
Published in print edition October, 2010

The term magnetic bearings refers to devices that provide stable suspension of a rotor. Because of the contact-less motion of the rotor, magnetic bearings offer many advantages for various applications. Commercial applications include compressors, centrifuges, high-speed turbines, energy-storage flywheels, high-precision machine tools, etc. Magnetic bearings are a typical mechatronic product. Thus, a great deal of knowledge is necessary for its design, construction and operation. This book is a collection of writings on magnetic bearings, presented in fragments and divided into six chapters. Hopefully, this book will provide not only an introduction but also a number of key aspects of magnetic bearings theory and applications. Last but not least, the presented content is free, which is of great importance, especially for young researcher and engineers in the field.